Quaternary Science Reviews 206 (2019) 141–149

Contents lists available at ScienceDirect

Quaternary Science Reviews

journal homepage: www.elsevier.com/locate/quascirev

A history of the modern Aral Sea (Central Asia) since the Late Pleistocene

G.S. Burr [a, *], Y.V. Kuzmin [b, c], S.K. Krivonogov [b, d], S.A. Gusskov [e], R.J. Cruz [f]

[a] National Taiwan University Research Center for Future Earth, Department of Geosciences, National Taiwan University, Taipei, 106, Taiwan
[b] Sobolev Institute of Geology and Mineralogy, Siberian Branch, Russian Academy of Sciences, Koptyug Ave. 3, Novosibirsk, 630090, Russia
[c] Laboratory of Mesozoic and Cenozoic Continental Ecosystems, Tomsk State University, Lenin Ave. 36, Tomsk, 634050, Russia
[d] Laboratory of Radiocarbon Method of Analyses, Novosibirsk State University, Pirogova St. 2, Novosibirsk, 630090, Russia
[e] Trofimuk Institute of Petroleum Geology and Geophysics, Siberian Branch, Russian Academy of Sciences, Koptyug Ave. 3, Novosibirsk, 630090, Russia
[f] Arizona AMS Laboratory, University of Arizona, Tucson, AZ, 85721-0081, USA

ARTICLE INFO

Article history:
Received 19 September 2018
Received in revised form
22 December 2018
Accepted 7 January 2019

Keywords:
Aral Sea
Late Pleistocene
Holocene
Sedimentology
Radiocarbon dating
Paleontology
Ostracods
Foraminifera
Central Asia

ABSTRACT

The catastrophic demise of the Aral Sea in the late twentieth century has stimulated significant international efforts to understand the geological, hydrological, and climatological controls on lake level at timescales ranging from years to millennia. Here we extend this time range to the Late Pleistocene with sedimentological, chronological and paleontological results from a core that dates from ca. 17.6 kyr cal BP. To our knowledge, this Aral Sea core (B-05-2009) is the oldest directly-dated sediment record with multiple late Pleistocene ^{14}C dates currently available from the region. The core shows that the modern Aral Sea formed at least as early as the end of the Last Glacial Maximum. The main source of water was most likely glacial meltwater from the Tian Shan, Pamir, and other distant mountain systems in the modern day Aral Sea watershed, carried by the Syr Darya and Amu Darya rivers. The Late Pleistocene section of the core contains ostracods and foraminifera throughout, providing evidence that the lake supported life since its inception. Our chronology suggests a relatively high average sedimentation rate at the onset of lake development, and a significant sedimentation hiatus around the time of the Pleistocene/Holocene boundary.

1. Introduction

The Aral Sea is a large endorheic lake situated in western Central Asia (Middleton, 2002). It is located within Kazakhstan and Uzbekistan; however, its watershed extends far beyond the boundaries of those countries, and includes parts of Tajikistan, Turkmenistan, Kyrgyzstan and Afghanistan (Fig. 1). The Aral Sea is fed primarily from the Amu Darya and Syr Darya rivers, both flowing from headwaters situated to the southeast in a mountainous region where the Pamir and Tian Shan range systems meet. The lake is well-known for the ecological collapse which occurred there in the late twentieth century. At that time the lake level dropped by about 26 m, and the lake surface extent and volume were reduced by ca. 90% (Micklin, 2014). This recent lake level fall was caused by the diversion of river water for industrial and agricultural purposes. However, it has also been demonstrated that regressions of nearly equal magnitude have occurred many times in the past (Boomer et al., 2009; Cretaux et al., 2013; Krivonogov et al., 2014). Following the ecological collapse of the Aral Sea region, a great deal of research has focused on the area in order to understand the history of the lake, and of the past 2000 years in particular (Nourgaliev et al., 2003; Sorrel et al., 2006, 2007; Austin et al., 2007; Oberhänsli et al., 2007; Píšková et al., 2009). These studies provide a quantitative understanding of natural lake level variations, from which the extent of human-made environmental impacts can be gauged.

Here we review what is known about the origin of the Aral Sea, then extend these findings with a nearly continuous record of lacustrine deposits, that includes sedimentological (grain size, sediment texture, sediment composition), paleontological (Ostracoda and Foraminifera), and chronological (radiocarbon dating) information. From these data we document the Late Pleistocene history (since ca. 17.6 kcal BP) at our site, identify the source of the

* Corresponding author.
E-mail address: burr@email.arizona.edu (G.S. Burr).

https://doi.org/10.1016/j.quascirev.2019.01.006
0277-3791/

Fig. 1. The Aral Sea watershed. Modified from Micklin (2014).

water, and describe its sedimentation history and microfaunal composition through time.

2. Background

2.1. Physical setting

There are three essential characteristics of the Aral Sea that make it unique as a continental archive of paleoclimate: 1) it is a relatively shallow terminal lake; 2) it is located in a semi-arid to arid ecotone; and 3) the catchment of the rivers supplying the Aral Sea bring the bulk of the water from more than 2000 km away, high in the mountains. The catchment area of the Aral Sea is vast, about 1,110,000 km^2 (United Nations Economic Commission for Europe, 2011), twice the size of France. The lake is situated in a broad depression that is bound on the west by the Usturt Plateau (Rubanov et al., 1987) and to the southeast by the Tian Shan and Pamir mountains (Rubanov et al., 1987; Boomer et al., 2000). Immediately to the south and east of the lake lie the Karakum and Kysylkum deserts. The precipitation rate across the basin increases from less than 50 mm yr^{-1} in the northwest to more than 1000 mm yr^{-1} in the southeast, where most of the water comes from (Zmijewski and Becker, 2014). This water is carried to the Aral Sea by two main rivers: the Syr Darya and the Amu Darya (Fig. 1). Both of these originate in the southeast. The Syr Darya forms in the western Tian Shan Mountains, at the confluence of the Naryn and Qoradaryo rivers, 2312 km from the Aral Sea. The headwaters of the Naryn and Qoradaryo rivers begin hundreds of km upstream from this confluence, so that some of the water carried by the Syr Darya may flow as far as 3000 km to reach the Aral Sea. The headwaters of the Amu Darya are in the Pamir Mountains, 2540 km from the Aral Sea. The Amu Darya also carries water from a portion of the northernmost Hindu Kush Mountains. In modern times, both the Syr Darya and Amu Darya rivers are fed primarily by glacial and snow meltwater (Aizen et al., 1995). Hence, on long time scales, the Aral Sea water budget is strongly leveraged by the climate in the distant mountainous catchment, rather than in the immediate vicinity of the lake. This distant sourcing of water is an essential characteristic that should always be borne in mind when considering the imprint of climate change on Aral Sea sediments. Additionally, lake level can be substantially affected by natural diversions of the river courses that supply water to the lake. This is especially true for the Amu Darya River whose contribution to the Aral Sea is controlled in part by tectonics and erosion on millennial timescales (Boomer et al., 2000; Krivonogov et al., 2014; Dodson et al., 2015).

2.2. A brief history of the Aral Sea

Despite the fact that the Amu Darya and Syr Darya rivers are very old and have fed the Caspian Basin since at least the middle Pliocene, their long-term relation to the Aral Sea as a terminal basin is still not fully understood. The structural basin in which the lake is situated falls within an active graben that dates to the Pliocene (Rubanov et al., 1987; Létolle and Mainguet, 1997) but the lake itself is much younger. The early history of the Aral Sea was considered in detail by Soviet and Russian researchers in the second half of the twentieth century (e.g., Kes, 1969, 1995; Rubanov et al., 1987), and their findings have been summarized in a number of review articles (e.g., Aladin and Plotnikov, 1995; Létolle and Mainguet, 1997; Boomer et al., 2000; Svitoch, 2010). According to those studies, the Aral Basin was dry during a long period of the middle Pleistocene, when wind erosion dominated the region. Several age estimates suggested a Late Pleistocene age for the lake. For example, Lopatin (1957) inferred an age of ca. 18.0 kyr based on a calculation of total volume. Chalov (1968) concluded that the Aral Sea could be as old as 139 ± 12 kyr, using U-series measurements on sediments, and that the Syr Darya River was its sole water source at the time. Létolle and Mainguet (1997), and Cretaux et al. (2013) both cited an extrapolated basal age of 11.0 ± 1.0 kyr BP for lacustrine sediments in a 3.5 m long core, described by Rubanov (1982). More recently, Krivonogov et al. (2010) reported a reservoir-corrected, calibrated ^{14}C age of 5.8–5.98 kcal BP for a shell sample collected from the base of an 8 m core (M1-2003), and an age of ca. 23.8 kcal BP from a gastropod shell from the sub-basal layer of core B1-2008 (Fig. 2).

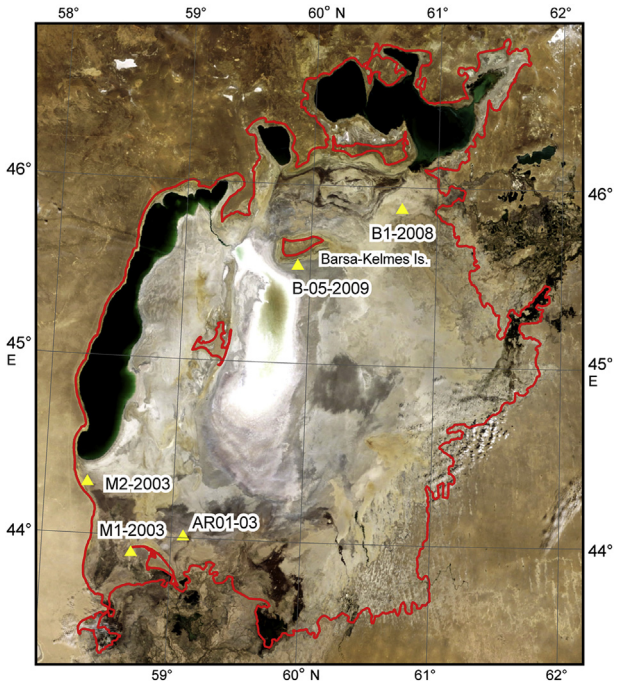

Fig. 2. MODIS (moderate-resolution imaging spectroradiometer) image (2009) of the Aral Sea. The red line shows the location of the AD 1960 shoreline. The locations of drill sites are marked with triangles. B05-2009 (this study), M1-2003 and B1-2008 (Krivonogov et al., 2010), M2-2003 (Guss'kov et al., 2011), AR1-03 (Boomer, 2012). (For interpretation of the references to colour in this figure legend, the reader is referred to the Web version of this article.)

Gus'kov et al. (2011) reported ^{14}C ages of 8.74 ± 0.95 kyr BP (16.6 m depth) and 8.54 ± 0.95 kyr BP (18.8 m depth) from core M2-2003, implying an age of ca. 10.0 kcal BP at the base of that core (20 m depth). Other studies reported a Holocene origin, based on sediment structure and ^{14}C dates (Nikolaev, 1991, 1995; Tarasov et al., 1996). Boomer (2012) reported a Late Pleistocene origin, based on a ^{14}C date of ca. 12,140 BP at 10.78 m depth, measured from ostracod shells (*Cyprideis torosa*) from his core: AR01-03 (Fig. 2). With this date, an extrapolated age of ca. 19,000 cal BP was proposed for the base of the 18 m-long sequence.

Recent work on the Aral Sea has focused on its Holocene and modern history (Boomer et al., 2009; Krivonogov et al., 2010; Cretaux et al., 2013). The most detailed lake level reconstructions are from the last 2000 years, when Aral Sea lake levels varied from about 10 m a.s.l. (Krivonogov et al., 2014) to a maximum of about 55 m a.s.l. (Reinhardt et al., 2008). The upper limit of this range is fixed by the elevation of a natural spillway from the Aral–Sarykamysh Basin to the Caspian Sea, as first noted by Berg (1908). Two protracted periods of low lake level occurred during the last two millennia, in addition to the modern one; with two relatively brief high lake level stands. Their timing has been established from several sources, including: historical records, archaeological information, sedimentological, and palynological data. Proposed causes for the marked variability within the last two millennia include climate change, transient river courses that periodically carried water away from the Aral Sea, and human impacts (Krivonogov et al., 2014).

3. Materials and methods

3.1. Coring site

The position of our Aral Sea core, B-05-2009, is 7 km south of the former Barsa-Kelmes Island (45.5° N, 59.9° E; 29.3 m a.s.l.) (Fig. 2). In AD 1960, the water depth at the core site exceeded 23 m, but is now exposed on the northern coast of what is currently referred to as the Eastern Large Aral Sea (Aladin et al., 2009). The coring location on the clayey vegetation-free plain was chosen as the farthest place from the shore of the former Barsa-Kelmes Island which could be safely reached by a track in 2009. Two years before, this site was underwater. The sediments were water-saturated, and the groundwater level was found at 0.6 m depth. The muddy plain extended ca. 10 km south-eastward toward the Aral Sea shore in that year.

3.2. Coring and sampling

Core B-05-2009 was taken in 2009 to a depth of 14.9 m using a portable drill system powered by an electric vibro-machine (jackhammer) with electric and hand-powered winches. The sampler was a variant of the Livingston piston corer allowing us to retrieve continuous and undisturbed sediment sections (11 lots in total), each 1 m long and 7.5 cm in diameter. The sediments below 11 m depth (four last lots) were retrieved using thinner slotted pipe, ca. 5 cm in diameter. Almost 100% or the core sediments were recovered. Less than 10 cm of unsorted and unconsolidated sediments that were introduced from the core walls during drilling, referred to here as “slime”, were registered in the upper parts of lots 2 and 3, and a 25 cm layer on top of lot 4. The sediment column was mechanically pressed out of the sampler, and hermetically packed into plastic film armored by plastic half-pipes for safe transport. The water-saturated sand layers and sediments from the 5 cm diameter pipe were cut into 10 and 5 cm lengths, respectively, and packed in plastic bags. The final length of the lots measured in the lab experienced a fractional extension/compression of 1.25 to 0.83, as compared with the drilling log; and the position of all of the samples and layer boundaries were recalculated to bring them in accord with the actual depths. The lots were split lengthwise, and a half-core was stored at the Sobolev Institute of Geology and Mineralogy, Siberian Branch of the Russian Academy of Sciences, in Novosibirsk, Russia. Another half-core was split in quarters and used for sedimentological and microfaunal analyses.

3.3. Sedimentological analysis

A grain size-based lithologic determination was performed, following the Russian State Standard Specification (GOST) 25100, which is in close agreement with the international ISO 14688 standard. The sampling interval was 3 cm. Five cm^3 of sediment was taken from each sampling interval, and dried at 80 °C to determine water content and related physical properties (wet and dry density, porosity, etc.). The dry samples were used to quantify the main sediment components (% dry wt.) in the following order: 1) water soluble (mostly chlorides); 2) hydrochloric acid soluble (mostly carbonates); 3) dispersed plant organic matter; and 4) terrigenous mineral fractions. The organic matter was estimated as loss-on-ignition at 450 °C. The mineral component was separated into clay, silt and sand fractions with a suspending-precipitating technique with a 10 s time lag. All measured parameters were integrated into three main sediment components: 1) organic component: 2) authigenic component (sum of chlorides and carbonates); and 3) terrigenous component (sum of sand, silt and clay). These parameters were used to determine changes in sediment composition and depositional environment along the core.

3.4. Microfaunal analysis

The study of ostracods and foraminifera preserved in lake

sediments can provide constraints on past environmental conditions, such as: temperature, salinity, and productivity (Lord et al., 2012; Rodriguez-Lazaro and Ruiz-Muñoz, 2012). Fossil ostracods from Aral Sea lake sediments have found wide use as paleoenvironmental proxies (Boomer, 2012; Boomer et al., 1996, 2000, 2009; Gus'kov et al., 2011), and foraminifera have also been described in Aral Sea sediments (Maier, 1974). Our intention is to use the presence of microfauna to show that the lake was continuously inhabited since it was first filled at our site, and to use the salinity tolerance of the ostracods to place bounds on past salinity (see discussion section).

From the quarter core used for microfaunal study, subsamples ranging from 65 to 190 g were taken at 10 cm intervals. Specimen counts were normalized by the weight of sediment. Microfossils were identified with the aid of an in-house reference collection at the Institute of Petroleum Geology and Geophysics (Novosibirsk, Russia) and basic works for identification of ostracods (Schornikov, 1973, 1974; Meisch, 2000) and foraminifera (Maier, 1974). For ostracods, the species and number of species within a particular interval were recorded. For the dominant taxa, growth stage (juvenile or adult), sex, dimensions, and degree of preservation were also determined. For foraminifera, the species, number of species within a particular interval, dimensions, and degree of preservation were determined.

3.5. Radiocarbon dating

Samples of *Caspiohydrobia* and *Cerastoderma* mollusc shells, and ostracod valves, were collected for ^{14}C dating at the Accelerator Mass Spectrometry (AMS) laboratory at the University of Arizona. Carbonate samples were dissolved in acid to release CO_2 gas. The CO_2 produced was then purified and reduced to graphite using iron powder as a catalyst and zinc as a reductant (Burr and Jull, 2010). A portion of the CO_2 was used to measure $\delta^{13}C$ values for a stable isotopic fractionation correction. The uncertainties in the ^{14}C dates due to counting errors, errors in the blank and random machine error were taken into account (Burr et al., 2007). The ^{14}C ages of the samples were corrected for a radiocarbon reservoir age effect of 168 ± 53 ^{14}C years (Kuzmin et al., 2007). That is the difference between the radiocarbon age of the shells living in the lake and the age of the contemporaneous atmosphere. The uncertainty in the radiocarbon reservoir age was propagated into the age uncertainty for every date. The corrected ^{14}C ages were calibrated with the OxCal 4.3 program (Bronk Ramsey, 2009) using the IntCal13 dataset (Reimer et al., 2013).

4. Results

4.1. Lithology

A sediment profile of core B-05-2009 is shown in Fig. 3. Lithologic types for most of the core include clay, a mixture of clay and sand (clayey sand), silt, silt with gypsum crystals, and sand of different grain sizes. In some cases, the sediment types grade from one to another, and in other cases we observe sharp boundaries, such as those surrounding the thin sand layers at depths of ca. 5.7 m and ca. 9.7 m. The boundaries between sediment layers are shown in Fig. 3. They reflect environmental changes which affected the character of the sediments transported to the sampling site. The dominance of fine-grained sediments with abrupt lithological changes is typical for sediments of the Aral Sea (e.g., Rubanov et al., 1987). Mollusc shells were common in many layers throughout the core, except the lowermost (sub-basal) part (depth of 10.7–14.9 m) which is represented by a compact loam with inclusions of gypsum crystals.

Sedimentological analysis shown in Fig. 3 display considerable variations in the proportions of the main sediment components. The terrigenous component dominates the Late Pleistocene portion of the core (66.3%), followed by the authigenic (24.0%) and organic fractions (9.7%). This is markedly different from the Holocene sediments, dominated by the authigenic component (50.4%), and followed by the terrigenous (28.1%) and organic (21.5%) components. Sharp fluctuations in these proportions represent significant and recurring changes in the sedimentation environment, especially evident in the Holocene. From the base of the core upward we observe strong terrigenous sedimentation that is gradually replaced by subequal terrigenous and authigenic sedimentation, and abruptly returns to dominant terrigenous sedimentation. The end of the Late Pleistocene is marked by a sharp drop in the proportion of terrigenous sediments (Fig. 3). We consider these features in the discussion below.

4.2. Chronology and Bayesian age model

Radiocarbon dates were obtained from a total of 23 samples, eight of them from the lower part of the core (5.25–9.95 m) (Table 1). All of the ^{14}C dates were measured on shell material, including molluscs (*Capiohydrobia* sp. and *Cerastoderma* sp.) and ostracods. A Bayesian age model was established using the OxCal 4.3 program (Bronk Ramsey, 2008, 2009, 2017), assuming only superposition of the samples in a coherent stratigraphic sequence (Table 1, Fig. 4) with two boundaries: 1) at the Pleistocene/Holocene transition (5.15–5.95 m depth), and 2) during the Late Holocene, where we observed a rapid change in radiocarbon age (ca. 2 m depth). The model age for the Pleistocene/Holocene boundary (12.9–10.4 kcal BP) agrees with the consensus age of ca. 11.7 kcal BP (Walker et al., 2009). The model age for the Late Holocene boundary was in the range 3.7–2.6 kcal BP (Table 1). The late Pleistocene part of the age model includes direct dates from ca. 17.0 to 13.0 kcal BP, with a projected age of 17.6 ka for the base of the lacustrine sediments in our core. The result for sample AA-90629 (Table 1) was excluded as an outlier because it's calibrated age was offset by more than 2000 calendar years from the consistent linear trend ($r^2 = 0.98$) of the other seven dates from the late Pleistocene dataset, and because the Bayesian model failed to converge when attempting to include this point. This shell may have been reworked, as it was deposited very near the Pleistocene/Holocene boundary. The sedimentation rate in the Pleistocene portion of the core is 1.0 mm yr^{-1}. The Holocene age model ranges from ca. 11.0 to 0 kcal BP with a sedimentation rate of 0.5 mm yr^{-1} ($r^2 = 0.98$) before the Late Holocene boundary, and 0.6 mm yr^{-1} ($r^2 = 0.99$) after the boundary. The coefficient of determination values (r^2) calculated for the three continuous segments of the age model reflect a high degree of linearity, and imply that the sedimentation rate at the site remained relatively constant, and the duration of possible hiatuses must be within the resolution of our age model (~100 years). The Pleistocene/Holocene transition is obvious in the sediment record at 5.43 m depth, where a sharp a transition from a low salinity to high salinity sedimentary environment is observed (Fig. 3).

4.3. Microfauna

To our knowledge, Boomer (2012) is the only work that presents microfaunal results from a long, well-dated Aral Sea core. The results presented here are consistent with the findings of Boomer (2012); however, the resolution of our radiocarbon (^{14}C) chronology is significantly more detailed.

The ostracod record of the B-05-2009 core is shown in Fig. 5. We identified 13 ostracod taxa in our core. In the Holocene part (depth

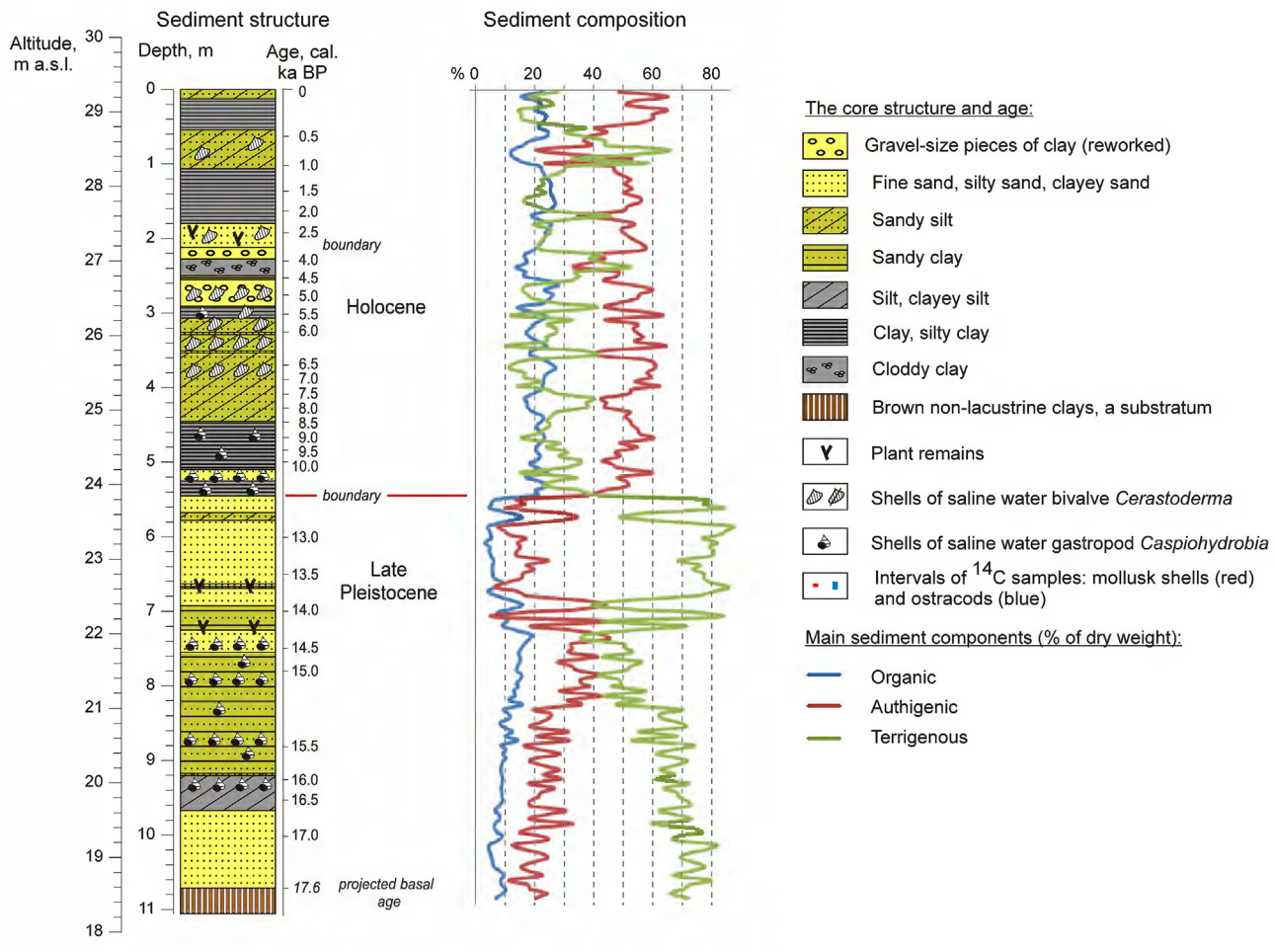

Fig. 3. Lithological divisions and proportions of main sediment components in the B-05-2009 core.

0.0–5.2 m), 12 taxa are observed, including (ordered by abundance): *Cyprideis torosa, Limnocythere inopinata, Leptocythere cymbula, Candona* sp., *Limnocythere vara, Darwinula stevensoni, Leptocythere relicta, Tyrrhenocythere amnicola, Ilyocypris caspiensis, Loxoconchissa immodulata, Candona neglecta?,* and *Cypridopsis aculeata*. These are dominated by *C. torosa*, which accounts for about 97% of all Holocene taxa. *L. inopinata* is the second most abundant taxa, accounting for about 1%. Boomer et al. (1996) describe the occurrence of 11 ostracod taxa in Holocene sediments from the Aral Sea, also with dominant euryhaline-tolerant *C. torosa* (Schornikov, 1973; Boomer et al., 1996). In the Late Pleistocene portion of the core (depth 5.2–10.4 m), we find seven taxa (ordered by abundance), including: *C. torosa, L. relicta, L. vara, L. inopinata, Plesiocypridopsis newtoni* (rare), *T. amnicola* (rare), *and Candona* sp. (rare). As in the Holocene portion, *C. torosa* dominates the microfaunal assemblage, accounting for about 98% of all taxa, with *L. relicta* as the second most abundant taxa (1.5%). Two foraminiferal species were identified in both the upper and lower portions of the core (Fig. 5): *Ammonia beccarii* and *Retroelphidium littorale* (also known as *Elphidium gunteri*). To our knowledge, these are the first reported foraminifera from the Aral Sea placed firmly in the Late Pleistocene (with age control). Near the bottom of the core (depth of 7.5–10.4 m), *R. littorale* was dominant and both species persisted in the lake since their introduction. Taphonomic observations show that foraminiferal complexes are autochthonous.

The oldest microfauna collected from the core date to about 17.3 kcal BP. After their appearance we find both ostracods and foraminifera throughout the core. These show that the Aral Sea was continuously inhabited since the lake first reached the lake level of the basal unit at our drill site.

5. Discussion

The modern climate of the Aral Sea region is distinctly continental, with hot summers and cold winters under semi-arid to arid conditions. The most significant moisture that eventually makes its way to the Aral-Caspian basin comes from the Atlantic Ocean, carried by the Westerlies. The highest precipitation occurs in spring and early summer, with a secondary precipitation peak during winter (Aizen et al., 1995). However, most of the precipitation that feeds the Aral Sea falls in a mountainous region to the southeast, and travels long distances (>2000 km) to reach the lake. This includes some of the highest mountains in the world, with peaks above 7000 m, in the Alay Range, western Tian Shan Mountains, Pamir Mountains, and northernmost Hindu Kush Mountains. Modern and past climate conditions within these mountain regions reflects an interplay between the Westerlies and the Siberian anticyclone, with a minor influence from the Asian monsoon, along the southern periphery of the Aral watershed (Shi, 2002; Abramowski et al., 2006; Chen et al., 2010).

Table 1
Bayesian model ^{14}C dates for the B-05-2009 core (shells and ostracods). Model ages were calculated with OxCal 4.3 (Bronk Ramsey, 2009) assuming superposition only (OxCal 4.3 "Sequence") and using the IntCal13 dataset (Reimer et al., 2013). Boundaries were calculated for an apparent hiatus between 1.95 and 2.13 m depth and at the Late Pleistocene/Holocene transition, 5.15–5.95 m depth. The date for AA90629 was rejected as an outlier, as discussed in the text.

AA #	depth (m)	^{14}C age, BP	±1σ	^{14}C age, reservoir corrected	±1σ	age range cal BP	cal BP ± 2σ	cal BP range, lower	cal BP range, upper	material dated
AA98085	0.35	327	34	159	63	150	77	−3	303	Ostracoda
AA98086	0.85	1050	42	882	68	790	53	684	896	Ostracoda
AA90617	1.00	1112	36	944	64	864	54	756	971	*Cerastoderma*
AA90618	1.92	2635	38	2467	65	2507	78	2351	2663	*Cerastoderma*
AA98087	1.95	2649	37	2482	65	2597	76	2445	2748	Ostracoda
model boundary								2589	3682	
AA90621	2.13	3559	47	3391	71	3657	90	3477	3836	*Cerastoderma*
AA90622	2.28	3871	47	3702	71	4047	100	3848	4246	*Cerastoderma*
AA98088	2.55	4218	47	4050	71	4477	110	4257	4696	Ostracoda
AA90623	2.58	4164	47	3992	71	4619	100	4419	4819	*Cerastoderma*
AA90624	2.85	4688	48	4520	72	5167	138	4891	5442	*Cerastoderma*
AA90625	3.00	4923	47	4752	71	5463	71	5321	5604	*Cerastoderma*
AA90626	3.30	5455	60	5287	80	6096	90	5916	6275	*Cerastoderma*
AA90627	3.62	5770	48	5602	72	6386	53	6281	6491	*Cerastoderma*
AA90628	3.71	5816	60	5648	80	6487	77	6333	6640	*Cerastoderma*
AA98089	5.15	9375	51	9207	74	10,397	80	10,236	10,557	Ostracoda
model boundary								10,401	12,950	
AA90629	*5.25*	*12,610*	*58*	*12,442*	*79*	*14,598*[a]	*208*	*14,182*	*15,013*	*Caspiohydrobia*
AA98090	5.95	11,295	55	11,127	76	12,962	83	12,797	13,127	Ostracoda
AA90630	7.47	12,544	57	12,376	78	14,491	194	14,103	14,879	*Caspiohydrobia*
AA90631	7.90	12,925	60	12,757	80	15,175	141	14,894	15,456	*Caspiohydrobia*
AA90632	8.78	13,116	58	12,948	79	15,502	128	15,246	15,758	*Caspiohydrobia*
AA90633	9.36	13,581	65	13,413	84	16,109	122	15,865	16,353	*Caspiohydrobia*
AA98224	9.45	13,764	85	13,596	100	16,441	149	16,142	16,739	Ostracoda
AA98225	9.95	14,178	82	14,010	98	16,950	180	16,591	17,309	Ostracoda

[a] Single calibrated age (exluded as an outlier from the Bayesian model).

Aizen et al. (1995) identified four types of rivers flowing from the Tian Shan Mountains: 1) rivers with mainly snow nourishment; 2) rivers with mainly glacial sources; 3) rivers with mainly rain nourishment (east Tian Shan); and 4) rivers with mainly ground water as a source (a minor component). The main water component in modern times is from melting of seasonal snow cover. Glacial runoff is also significant, and in modern times accounts for 15–20% of the total river runoff volume. It can reach 35% during dry years

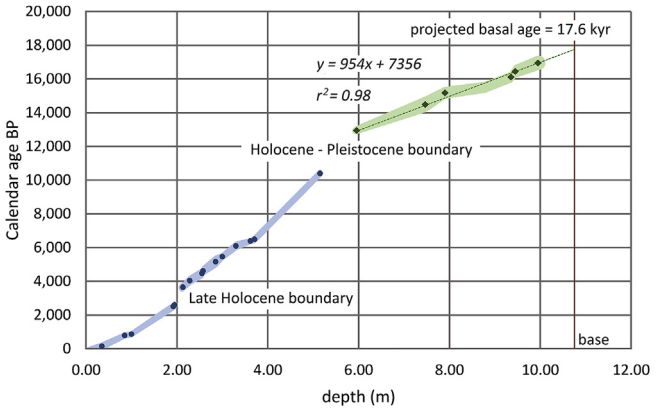

Fig. 4. Bayesian age model for the B-05-2009 core (shells and ostracods). Model ages were calculated with OxCal 4.3 (Bronk Ramsey, 2009) assuming superposition only (OxCal 4.3 "Sequence"), using the IntCal13 dataset (Reimer et al., 2013). Boundaries were calculated for an apparent hiatus between 1.95 and 2.13 m depth and at the Late Pleistocene/Holocene transition, 5.15–5.95 m depth. The date for AA90629 was rejected as an outlier, as discussed in the text. The shaded areas about the curves show the 2σ calendar age uncertainties in the age model. The dashed line is the linear regression line for the Pleistocene portion of the model and projects to the age of the base of the section at about 17.6 kcal BP. The equation of the regression line and coefficient of determination are shown.

(Aizen et al., 1995). This is reflected in the large number of modern and remnant glacial lakes in the headwaters of the Amu Darya, 73% of which are situated above 4000 m a.s.l. (Mergili et al., 2013). The basal date of our Aral core follows closely the age of the retreat of mid-latitude glaciers from around the globe (Schaefer et al., 2006), and suggests a glacial origin for the water that filled the lake at that time.

Numerous studies have documented LGM glacial advances in the mountainous catchment of the Aral Sea. Although LGM advances in the region were not as large as those during MIS3/4 (Shi, 2002; Koppes et al., 2008), they still produced easily recognizable and widespread glacial deposits (Zech et al., 2005, 2013; Abramowski et al., 2006; Narama et al., 2007). Eight examples that date from ca. 18–23 cal kyr, are listed in Table 2. The extent of glaciation that occurred at these sites is reflected in their equilibrium line altitude (ELA) values - the altitude where the accumulation zone of a glacier is balanced by its ablation zone. Glacial advances produce ELA depressions, and these reflect the relative magnitude of an advance. Lifton et al. (2014) dated LGM glacial deposits from the Inylchek and Sary-Dzaz valleys (79°N, 42°N), on the eastern margin of the Aral Sea watershed, using ^{10}Be and ^{26}Al, and determined an ELA depression (ΔELA) of 225 m, using the toe-to-summit altitude method. They compared this value to ELA depressions from other Aral watershed sites, that ranged from 260 m (Abramowski et al., 2006) and 275 m (Zech, 2012), to 350–465 m (Narama et al., 2007, 2009). Hence, LGM glaciation in the Aral watershed was significant and widespread. The timing determined in these glacial studies agree well with the basal date of our core, and point to a water source that can explain the terrigenous sedimentation that we observe following the Late Pleistocene onset of sedimentation (Fig. 3). LGM ice advances served to store water as ice in the mountainous Aral watershed, and subsequent deglaciation provided for a steady flow of water and sediment into the Aral

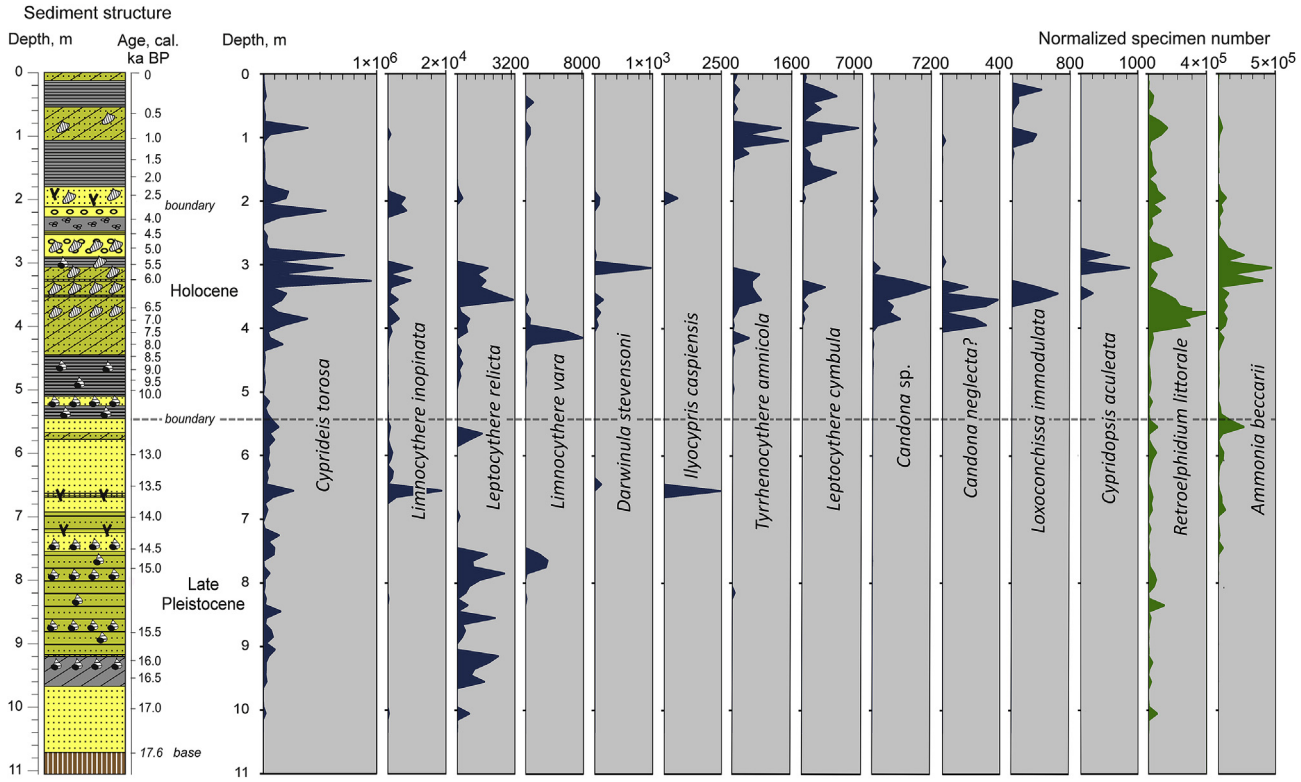

Fig. 5. The microfaunal record from core B-05-2009. Ostracods are shown in blue and foraminifera are shown in green. (For interpretation of the references to colour in this figure legend, the reader is referred to the Web version of this article.)

Table 2
Dated LGM glacial deposits from the Aral Sea catchment region.

Site/Mountain Range	Location	LGM glacial ages	Reference
Lake Yashilkul/Pamir Mountains	37.8°N, 72.8°E	~19 cal kyr	Zech et al. (2005)
		~18–20 cal kyr	Abramowski et al. (2006)
Aksu Valley/Turkestan Range	39.6° N, 69.5° E	~18–20 cal kyr	Abramowski et al. (2006)
Ailuitek Pass area/Pamir Mountains	38.6° N, 72.9° E	~18–20 cal kyr	Abramowski et al. (2006)
Kol-Uchkol river valley	37.7° N, 73.7° E	~23-21 cal kyr	Abramowski et al. (2006)
Gurumdy river valley/Southern Alichur Range	37.6° N, 73.9° E	~21–23, ~18–20 cal kyr	
Terskey-Alatoo Range	42° N, 76.5° E	~21 cal kyr	Narama et al. (2007)
At-Bashy Range	41.2° N, 76.5° E	~18 cal kyr	Narama et al. (2009)
	40.8° N, 75.5° E	~21 cal kyr	Zech (2012)
Gissar Range	39.0° N, 68.2° E	~20 cal kyr	Zech et al. (2013)

Ages from Abramowski et al. (2006) taken from their summary figure (Figure 11).

basin for many years.

The proportions of Late Pleistocene sediment components in our core are distinctly different from those observed in the Holocene. In general, the Holocene is dominated by authigenic sediments with consistently low sedimentation rates (0.5–0.6 mm yr^{-1}), while Late Pleistocene sediments are dominated by terrigenous sediments deposited under a relatively high sedimentation rate (1 mm yr^{-1}). The glacial meltwater supplied at the end of the LGM from the mountains to the southeast apparently provided a constant flow of water from about 17.6 to 15.3 kcal BP (10.7 m–8.3 m depth), when the terrigenous sediment fraction was consistently >70%. This observation agrees with the findings of Boomer (2012), who suggested that a persistent change in oxygen isotope ratios from ostracods deposited during the first two thousand years of the Aral Sea are indicative of glacial meltwater. From about 15.3 to 14.5 kcal BP (8.3 m–7.5 m depth), the terrigenous sediment fraction fell to as low as 50%, with a commensurate increase in the authigenic fraction, of up to 40%, and a decrease in the organic sediment component from >10% to <5% (Fig. 3). This points to a time of increased salinity in the lake which culminated in the disappearance of the minor ostracod taxa *L. relicta* and *L. vara* (Fig. 5). From 14.5 to 14.0 kcal BP (7.5–7.0 m) *C. torosa* was the only ostracod taxon present, while the foraminifera *R. littorale* and *A. beccarii* persisted in reduced numbers (Fig. 5). Following an unstable period, with rapidly varying proportions of sediment components, the terrigenous fraction subsequently climbed to more than 80% and stayed there, from about 13.8 to 13.0 kcal BP (6.9–5.9 m depth). A hiatus followed between the Late Pleistocene and the Holocene (Table 1, Fig. 4). When sedimentation resumed, the authigenic fraction became dominant, and the average sedimentation rate fell. A detailed account of Holocene sedimentation, including multiple cores will be discussed in a future article.

Ostracod *C. torosa* established itself as an early and persistent inhabitant at our coring site, and survived both sediment hiatuses

and highly variable sedimentation conditions during the Late Pleistocene. This is likely due to *C. torosa's* very large salinity tolerance, 0–70‰, much larger than any marine ostracod (De Deckker, 1981). This salinity tolerance also allowed *C. torosa* to persist in the lake throughout large Holocene lake level fluctuations (e.g., Krivonogov et al., 2014; Boomer et al., 2009), and most recently, *C. torosa* was the only ostracod taxon to survive the severe desiccation of the lake in the latter half of the twentieth century (Boomer et al., 1996). Other ostracod taxa are freshwater–brackish types (salinity of 0–10‰) and brackish–marine types (10–35‰) (Schornikov, 1973, 1974; Boomer et al., 1996). Although we cannot use the weighted number of *C. torosa* specimens alone to infer periods of high salinity, very high proportions of *C. torosa*, coincident with an absence of less salinity-tolerant taxa, and coupled with a relatively high authigenic sediment component argue for very saline conditions, which is what we observe between 14.5 and 14.0–kcal BP.

6. Conclusions

We describe a 10.4 m-long record of Aral Sea microfauna, from core B-05-2009, firmly dated to 17.6 cal kyr BP. This is a new estimate of the minimum age of the modern Aral Sea based on direct evidence that include 23 δ^{13}C-corrected, and reservoir-age corrected AMS ^{14}C dates. A Bayesian age model shows consistent inferred sedimentation rates from the lower (depth 6.0–10.0 m) and upper (depth 0.0–5.2 m) parts of the core, with a sedimentation change between the Late Pleistocene and Holocene, and a hiatus in the late Holocene at our site. The elevation of the dry Aral Sea bottom, where core B-05-2009 was taken, is 29.3 m above the Baltic datum. This corresponds to a depth of ca. 24 m in relation to the AD 1960 level of +53 m. The high degree of linearity in the age model, combined with the lacustrine microfauna throughout the core, suggests that the lake level in the past never experienced protracted low lake levels below ca. +10.0 m in the Late Pleistocene, within the resolution of our age model (~100 years). Our results are consistent with previous estimates of a maximal Aral Sea regression of ca. +30 to +32 m (Nikolaev, 1995; Boomer et al., 2000) for the period 17.6–13.0 kyr cal BP.

We show that the style and rate of sedimentation in the Late Pleistocene was distinctly different from the Holocene. The Late Pleistocene can be broadly divided into three stages: 1) primarily terrigenous (>70%) sedimentation from about 17.6 to 15.3 kcal BP, 2) subequal terrigenous and authigenic sedimentation from about 15.3 to 13.8 kcal BP, under relatively saline conditions (especially 14.5 to 14.0 kcal BP), and 3) primarily terrigenous (>80%) sedimentation from 13.8 to 13.0 kcal BP. The widespread retreat of LGM glaciers throughout the headwater region of the Aral Sea watershed are concurrent with the basal age of our core site, supporting the interpretation that the lake was probably initially filled with glacial meltwater during a time of global warming, and the strong terrigenous sedimentation in the Late Pleistocene suggests that this source supplied a constant supply of water for thousands of years.

Acknowledgments

We are indebted to Mr. E. Zhakov for his contribution to the microfaunal analyses. This research was funded by the joint US CRDF – Russian RFFI Project "Environmental history of the Aral Sea in the last 10,000 years: natural and anthropogenic components" in 2008–2010 (grants RUG1-2921-NO-07 and 08-05-91105, respectively); it was also supported by State Assignment Project (0330-2016-2018), the Tomsk State University Competitiveness Improvement Program and a Taiwan Ministry of Education Grant (NTU-107L9010). The work was conducted under the State Aassignment of the IGM SB RAS and under the framework of the project "Effective use of the AMS radiocarbon analysis in Earth Sciences" of the SB RAS Integration Program. We used the laboratory facilities of the Center of Sample Preparation of the Novosibirsk State University supported by the Ministry of Science and Higher Education of the Russian Federation (project # 14.Y26.31.0018). We are very grateful to Dr. A. Mackay and Dr. A.J.T. Jull for their constructive criticisms of the manuscript.

References

Abramowski, U., Bergau, A., Seebach, D., Zech, R., Glaser, B., Sosin, P., Kubik, P.W., Zech, W., 2006. Pleistocene glaciations of Central Asia: results from ^{10}Be surface exposure ages of erratic boulders from the Pamir (Tajikistan), and the Alay–Turkestan range (Kyrgyzstan). Quat. Sci. Rev. 25, 1080–1096. https://doi.org/10.1016/j.quascirev.2005.10.003.

Aizen, V.B., Aizen, E.M., Melack, J.M., 1995. Climate, snow cover, glaciers, and runoff in the Tien Shan, Central Asia. Water Resour. Bull. 31, 1113–1129. https://doi.org/10.1111/j.1752-1688.1995.tb03426.x.

Aladin, N.V., Plotnikov, I.S., 1995. Changes in the Aral Sea level: paleolimnological and archaeological evidences. part 1. In: Alimov, A.F., Aladin, N.V. (Eds.), Biological and Environmental Problems of the Aral Sea and Aral Region. Proceedings of the Zoological Institute, Russian Academy of Sciences, vol. 262. Zoological Institute, St.-Petersburg, pp. 17–46 (in Russian).

Aladin, N.V., Plotnikov, I.S., Micklin, P., Ballatore, T., 2009. Aral Sea: water level, salinity and long-term changes in biological communities of an endangered ecosystem – past, present and future. Nat. Resour. Environ. Issues 15. Article 36.

Austin, P., Mackay, A., Palagushkina, O., Leng, M., 2007. A high-resolution diatom-inferred palaeoconductivity and lake level record of the Aral Sea for the last 1600 yr. Quat. Res. 67, 383–393. https://doi.org/10.1016/j.yqres.2007.01.009.

Berg, L.S., 1908. The Aral Sea. An Experience of Physical–Geographical Monograph. Stasyulevich Publishers, St.-Petersburg (in Russian).

Boomer, I., 2012. Ostracoda as indicators of climatic and human-influenced changes in the late quaternary of the ponto-caspian region (aral, caspian and black seas). In: Horne, D.J., Holmes, J., Rodriguez-Lazaro, J., Viehberg, F.A. (Eds.), Ostracoda as Proxies for Quaternary Climate Change. Elsevier Science, Amsterdam, pp. 205–215. https://doi.org/10.1016/B978-0-444-53636-5.00012-3.

Boomer, I., Watley, R., Aladin, N.V., 1996. Aral Sea ostracoda as environmental indicators. Lethaia 29, 77–85. https://doi.org/10.1111/j.1502-3931.1996.tb01840.x.

Boomer, I., Aladin, N., Plotnikov, I., Whatley, R., 2000. The palaeolimnology of the Aral Sea: a review. Quat. Sci. Rev. 19, 1229–1278. https://doi.org/10.1016/S0277-3791(00)00002-0.

Boomer, I., Wünnemann, B., Mackay, A.W., Austin, P., Sorrel, P., Reinhardt, C., Keyser, D., Guichard, F., Fontugne, M., 2009. Advances in understanding the late Holocene history of the Aral Sea region. Quat. Int. 194, 79–90. https://doi.org/10.1016/j.quaint.2008.03.007.

Bronk Ramsey, C., 2008. Deposition models for chronological records. Quat. Sci. Rev. 27 (1–2), 42–60. https://doi.org/10.1016/j.quascirev.2007.01.019.

Bronk Ramsey, C., 2009. Bayesian analysis of radiocarbon dates. Radiocarbon 51 (1), 337–360. https://doi.org/10.1017/S0033822200033865.

Bronk Ramsey, C., 2017. Methods for summarizing radiocarbon datasets. Radiocarbon 59 (6), 1809–1833. https://doi.org/10.1017/RDC.2017.108.

Burr, G.S., Jull, A.J.T., 2010. Accelerator Mass Spectrometry for radiocarbon research. In: Beauchemin, D., Matthews, D.E. (Eds.), The Encyclopedia of Mass Spectrometry. Volume 5, Elemental and Isotope Ratio Mass Spectrometry. Elsevier Science, Amsterdam, pp. 656–669.

Burr, G.S., Donahue, D.J., Tang, Yu, Beck, J.W., McHargue, L., Biddulph, D., Cruz, R., Jull, A.J.T., 2007. Error analysis at the NSF-Arizona AMS facility. Nucl. Instrum. Methods Phys. Res. B 259, 149–153. https://doi.org/10.1016/j.nimb.2007.01.301.

Chalov, P.I., 1968. The Non-equilibrium Uranium Dating. Ilim, Frunze (in Russian).

Chen, F.-H., Chen, J.-H., Holmes, J., Boomer, I., Austin, P., Gates, J.B., Wang, N.-L., Brooks, S.J., Zhang, J.-W., 2010. Moisture changes over the last millennium in arid central Asia: a review, synthesis and comparison with monsoon region. Quat. Sci. Rev. 29, 1055–1068. https://doi.org/10.1016/j.quascirev.2010.01.005.

Cretaux, J.-F., Létolle, R., Bergé-Nguyen, M., 2013. History of Aral Sea level variability and current scientific debates. Glob. Planet. Chang. 110, 99–113. https://doi.org/10.1016/j.gloplacha.2013.05.006.

De Deckker, P., 1981. Ostracods of athalassic saline lakes. Hydrobiologia 81, 131–144. https://doi.org/10.1007/978-94-009-8665-7_10.

Dodson, J., Betts, A.V.G., Amirov, S.S., Yagodin, V.N., 2015. The nature of fluctuating lakes in the southern Amu-Dar'ya delta. Palaeogeogr. Palaeoclimatol. Palaeoecol. 437, 63–73. https://doi.org/10.1016/j.palaeo.2015.06.026.

Gus'kov, S.A., Zhakov, E.Y., Kuzmin, Y.V., Krivonogov, S.K., Burr, G.S., Kanygin, A.V., 2011. New data on evolution of the Aral Sea and its relations with the west siberian plain through the Holocene. Dokl. Earth Sci. 437, 460–463.

Kes, A.S., 1969. The main stages in the development of the Aral Sea. In: Geller, S.Y. (Ed.), Problem of the Aral Sea. Nauka, Moscow, pp. 160–172 (in Russian).

Kes, A.S., 1995. Chronicle of the Aral Sea and the sub-aral region. Geojournal 35 (1), 7–10.

Koppes, M., Gillespie, A.R., Burke, R.M., Thompson, S.C., Stone, J., 2008. Late quaternary glaciation in the Kyrgyz tien Shan. Quat. Sci. Rev. 27, 846–866. https://

doi.org/10.1016/j.quascirev.2008.01.009.
Krivonogov, S.K., Kuzmin, Y.V., Burr, G.S., Gusskov, S.A., Khazin, L.B., Zhakov, E.Y., Nurgizarinov, A.N., Kurmanbaev, R.K., Kenshinbay, T.I., 2010. Environmental changes of the Aral Sea (central Asia) in the Holocene – major trends. Radiocarbon 52, 555–568. https://doi.org/10.1017/S0033822200045598.
Krivonogov, S.K., Burr, G.S., Kuzmin, Y.V., Gusskov, S.A., Kurmanbaev, R.K., Kenshinbay, T.I., Voyakin, D.A., 2014. The fluctuating Aral Sea: a multidisciplinary-based history of the last two thousand years. Gondwana Res. 25, 284–300. https://doi.org/10.1016/j.gr.2014.02.004.
Kuzmin, Y.V., Nevesskaya, L.A., Krivonogov, S.K., Burr, G.S., 2007. Apparent ^{14}C ages of the 'pre-bomb' shells and correction values (R, ΔR) for caspian and aral seas (central Asia). Nucl. Instrum. Methods Phys. Res. B 259, 463–466. https://doi.org/10.1016/j.nimb.2007.01.187.
Létolle, R., Mainguet, M., 1997. History of the Aral Sea (central Asia) since the most recent maximum glaciation. Bull. Geol. Soc. France 168, 387–398 (in French).
Lifton, N., Beel, C., Hättestrand, Kassab C., Rogozhina, I., Heermance, R., Oskin, M., Burbank, D., Blomdin, R., Gribenski, N., Caffee, M., Goehring, B.M., Heyman, J., Ivanov, M., Li, Y.N., Li, Y.K., Petrakov, D., Usubaliev, R., Codilean, A.T., Chen, Y.X., Harbor, J., Stroeven, A.P., 2014. Constraints on the late Quaternary glacial history of the Inylchek and Sary-Dzaz valleys from in situ cosmogenic ^{10}Be and ^{26}Al, eastern Kyrgyz Tian Shan. Quat. Sci. Rev. 101, 77–90. https://doi.org/10.1016/j.quascirev.2014.06.032.
Lopatin, G.V., 1957. Structure of the Amu Darya delta and its formation history. Proc. Lake Res. Lab. USSR Acad. Sci. 4, 5–34 (in Russian).
Lord, A.R., Boomer, I., Brouwers, E., Whittaker, J.E., 2012. Ostracod taxa as paleoclimate indicators in the Quaternary. In: Horne, D.J., Holmes, J., Rodriguez-Lazaro, J., Viehberg, F.A. (Eds.), Ostracoda as Proxies for Quaternary Climate Change. Elsevier Science, Amsterdam, pp. 37–45. https://doi.org/10.1016/B978-0-444-53636-5.00003-2.
Maier, E.M., 1974. Foraminiferida. In: Mordukhai-Boltovskoi, F.D. (Ed.), Atlas of Invertebrates of the Aral Sea. Pishchevaya Promyshlennost Publishers, Moscow, pp. 12–36 (in Russian).
Meisch, C., 2000. Ostracoda (Süßwasserfauna von Mitteleuropa, Bd. 8/3. G. Fischer, Stuttgart.
Mergili, M., Müller Johannes, P., Schneider Jean, F., 2013. Spatio-temporal development of high-mountain lakes in the headwaters of the Amu Darya river (central Asia). Glob. Planet. Chang. 107, 13–24. https://doi.org/10.1016/j.gloplacha.2013.04.001.
Micklin, P., 2014. Introduction to the Aral Sea and its region. Chapter 2. In: Micklin, P., Aladin, N.V., Plotnikov, I.S. (Eds.), The Aral Sea. The Devastation and Partial Rehabilitation of a Great Lake. Springer, New York, pp. 15–40.
Middleton, N., 2002. The Aral Sea. In: Shahgedanova, M. (Ed.), The Physical Geography of Northern Eurasia. Oxford University Press, Oxford, pp. 497–510.
Narama, C., Kondo, R., Tsukamoto, A., Kajiura, T., Ormukov, C., Abdrakhmatov, K., 2007. OSL dating of glacial deposits during the last glacial in the terskey-alatoo range, Kyrgyz Republic. Quat. Geochronol. 2, 249–254. https://doi.org/10.1016/j.quageo.2006.06.007.
Narama, C., Kondo, R., Tsukamoto, S., Kajiura, T., Duishonakunov, M., Abdrakhmatov, K., 2009. Timing of glacier expansion during the last glacial in the inner tien Shan, Kyrgyz Republic by OSL dating. Quat. Int. 199, 147–156. https://doi.org/10.1016/j.quaint.2008.04.010.
Nikolaev, S.D., 1991. The development of the Aral Sea from oxygen isotope data. In: Sevastyanov, D.V., Mamedov, E.D., Rumyantsev, V.A. (Eds.), History of Lakes Sevan, Issyk Kul, Balkhash, Zaysan and Aral. Nauka, Leningrad, pp. 246–249 (in Russian).
Nikolaev, S.V., 1995. Isotope Paleogeography of Intracontinental Seas. VNIRO Publishers, Moscow (in Russian).
Nourgaliev, D.K., Heller, F., Borisov, A.S., Hajdas, I., Bonani, G., Iassonov, P.G., Oberhänsli, H., 2003. Very high resolution paleosecular variation record for the last 1200 years from the Aral Sea. Geophys. Res. Lett. 30 (17), 41–44. https://doi.org/10.1029/2003GL018145.
Oberhänsli, H., Boroffka, N., Sorrel, P., Krivonogov, S., 2007. Climate variability during the past 2,000 years and past economic and irrigation activities in the Aral Sea basin. Irrigat. Drain. Syst. 21 (3–4), 167–183. https://doi.org/10.1007/s10795-007-9031-5.
Píšková, A., Grygar, T., Veselá, J., Oberhänsli, H., 2009. Diatom assemblage variations in the Aral Sea core C2/2004 over the past two millennia. Fottea 9, 333–342. https://doi.org/10.5507/fot.2009.032.
Reinhardt, C., Wünnemann, B., Krivonogov, S.K., 2008. Geomorphological evidence for the late Holocene evolution and the Holocene lake level maximum of the Aral Sea. Geomorphology 93, 302–315. https://doi.org/10.1016/j.geomorph.2007.03.002.
Reimer, P.J., Bard, E., Bayliss, A., Beck, J.W., Blackwell, P.G., Bronk Ramsey, C., Buck, C.E., Cheng, H., Edwards, R.L., Friedrich, M., Grootes, P.M., Guilderson, T.P., Haflidason, H., Hajdas, I., Hatté, C., Heaton, T.J., Hogg, A.G., Hughen, K.A., Kaiser, K.F., Kromer, B., Manning, S.W., Niu, M., Reimer, R.W., Richards, D.A., Scott, E.M., Southon, J.R., Turney, C.S.M., van der Plicht, J., 2013. IntCal13 and Marine13 radiocarbon age calibration curves 0–50,000 years cal BP. Radiocarbon 55, 1869–1897. https://doi.org/10.2458/azu_js_rc.55.16947.
Rodriguez-Lazaro, J., Ruiz-Muñoz, F., 2012. A general introduction to ostracods: morphology, distribution, fossil record and applications. Dev. Quat. Sci. 17, 1–14. https://doi.org/10.1016/B978-0-444-53636-5.00001-9.
Rubanov, V.I., 1982. About the layer of plant remains in bottom sediments of the Aral Sea. Doklady Acad. Sci. USSR 264, 927–929 (in Russian).
Rubanov, I.V., Ischniyazov, D.P., Baskakova, M.A., 1987. The Geology of the Aral Sea. Fan Publishers, Tashkent (in Russian).
Schaefer, J.M., Denton, G.H., Barrell, D.J.A., Ivy-Ochs, S., Kubik, P.W., Andersen, B.G., Phillips, F.M., Lowell, T.V., Schlüchter, C., 2006. Near-synchronous interhemispheric termination of the last glacial maximum in mid-latitudes. Science 312, 1510–1513. https://doi.org/10.1126/science.1122872.
Schornikov, E.I., 1973. Ostracoda of the Aral Sea. Zoologichesky Zhurnal 52, 1304–1314 (in Russian with English abstract).
Schornikov, E.I., 1974. Ostracoda. In: Mordukhai-Boltovskoi, F.D. (Ed.), Atlas of Invertebrates of the Aral Sea. Pishchevaya Promyshlennost Publishers, Moscow, pp. 180–199 (in Russian).
Shi, Y., 2002. Characteristics of late quaternary monsoonal glaciation on the Tibetan plateau and in east Asia. Quat. Int. 97/98, 79–91. https://doi.org/10.1016/S1040-6182(02)00053-8.
Sorrel, P., Popescu, S.-M., Head, M.J., Suc, J.P., Klotz, S., Oberhänsli, H., 2006. Hydrographic development of the Aral Sea during the last 2000 years based on a quantitative analysis of dinoflagellate cysts. Palaeogeogr. Palaeoclimatol. Palaeoecol. 234, 304–327.
Sorrel, P., Popescu, S.-M., Klotz, S., Suc, J.-P., Oberhänsli, H., 2007. Climatic variability in the Aral Sea basin (Central Asia) during the late Holocene based on vegetation changes. Quat. Res. 67, 357–370. https://doi.org/10.1016/j.yqres.2006.11.006.
Svitoch, A.A., 2010. Paleogeographical history of the Aral Sea. In: Kostianoy, A.G., Kosarev, A.N. (Eds.), The Aral Sea Environment. Springer, Berlin & Heidelberg, pp. 11–30.
Tarasov, P.E., Pushenko, M.Y., Harrison, S.P., Saarse, L., Andreev, A.A., Aleshinskaya, Z.V., Davydova, N.N., Dorofeyuk, N.I., Efremov, YuV., Elina, G.A., Elovicheva, Y.K., Filimonova, L.V., Gunova, V.S., Khomutova, V.I., Kvavadze, E.V., Neustrueva, I.Y., Pisareva, V.V., Sevastyanov, D.V., Shelekhova, T.S., Subetto, D.A., Uspenskaya, O.N., Zernitskaya, V.P., 1996. Lake Status Records from the Former Soviet Union and Mongolia. Documentation of the Second Version of the Data Base, vol. 5. NOAA Paleoclimatology Publications Series Report, Boulder, CO. NOAA/NGDC Paleoclimatology Program.
United Nations Economic Commission for Europe, Second Assessment of Transboundary Rivers, Lakes and Groundwaters, 2011. Aral Sea and other transboundary waters in central Asia. In: Second Assessment of Transboundary Rivers, Lakes and Groundwaters. United Nations, New York and Geneva, pp. 107–130.
Walker, M., Johnsen, S., Rasmussen, S.O., Popp, T., Steffensen, J.-P., Gibbard, P., Hoek, W., Lowe, J., Andrews, J., Björck, S., Cwynar, L.C., Hughen, K., Kershaw, P., Kromer, B., Litt, T., Lowe, D.J., Nakagawa, T., Newnham, R., Schwander, J., 2009. Formal definition and dating of the GSSP (global stratotype section and point) for the base of the Holocene using the Greenland NGRIP ice core, and selected auxiliary records. J. Quat. Sci. 24, 3–17. https://doi.org/10.1002/jqs.1227.
Zech, R., 2012. A late Pleistocene glacial chronology from the Kitschi-Kurumdu Valley, Tien Shan (Kyrgyzstan), based on ^{10}Be surface exposure dating. Quat. Res. 77, 281–288. https://doi.org/10.1016/j.yqres.2011.11.008.
Zech, R., Abramowski, U., Glaser, B., Sosin, P., Kubik, P.W., Zech, W., 2005. Late Quaternary glacial and climate history of the Pamir Mountains derived from cosmogenic ^{10}Be exposure ages. Quat. Res. 64, 212–220. https://doi.org/10.1016/j.yqres.2005.06.002.
Zech, R., Röhringer, I., Sosin, P., Kabgov, H., Merchel, S., Akhmadaliev, S., Zech, W., 2013. Late Pleistocene glaciations in the Gissar Range, Tajikistan, based on ^{10}Be surface exposure dating. Palaeogeogr. Palaeoclimatol. Palaeoecol. 369, 253–261. https://doi.org/10.1016/j.palaeo.2012.10.031.
Zmijewski, K., Becker, R., 2014. Estimating the effects of anthropogenic modification on water balance in the Aral Sea watershed using GRACE: 2003–12. Earth Interact. 18 https://doi.org/10.1175/2013EI000537.1. Paper 3.